Roll deformation during blade coating

DOUGLAS W. BOUSFIELD, MIKAEL RIGDAHL, AND MAGNUS WIKSTRÖM

ABSTRACT

The deformation of a fiber web and a rubber-covered roll is modeled in conjunction with the fluid dynamics during blade coating. Deformations are calculated with a finite element method and a simple spring model. The simple spring model for the solid deformation is inadequate for deformations over 5 μm. As deformation increases, a single pressure peak develops a shoulder and eventually develops into a double pressure peak. Further deformation leads to a case where no solution to both equations can be found. This condition may represent an industrial blade coater for which there is a lower limit to the coat weight.

Application: *This analysis characterizes how the deformation of rubber and paper affect the steady operation of the blade coater. Operational limits may be defined by this work.*

A PAPER OR PAPERBOARD PRODUCT may be coated to improve the optical and printing properties. Supported by a rubber-covered roll, the paper web passes at high speed under a blade that takes off the excess coating. After drying, a thin and porous coating layer covers the paper surface. The blade coating operation is often performed at a speed of 15 m/s or higher. A number of control and operational problems are associated with the process, especially at a high speed or at a high concentration of coating solids.

One problem is that the paper and the rubber roll bend out of shape during blade coating. This deformation has an impact on the coat weight uniformity and on the general operation of the process. Previous research has shown that the geometry of the blade and roll in its fine details determines the forces acting on the blade. Some have speculated on the geometry of the roll deformation, but this aspect has not been closely studied.

Our research reported here centers on the question of how the coating performance is affected as the coating substrate deforms under pressure applied by the blade. In this work, we have calculated the pressure field under the blade in conjunction with the stress field in the paper and rubber roll. Our results may prove helpful in the ongoing effort to analyze probable responses in the blade coater's performance when variations in process parameters are being considered.

PREVIOUS RESEARCH

Over the last few decades, Turai, Eklund and Kahila, Kuzmak, and others have analyzed various aspects of the blade coating process (*1–3*). The lubrication flow under the blade is an important aspect of the coating operation. The coat weight is controlled with blade loading, where the blade is supported by the lubrication flow under it. The inertia of the flow striking the blade is an important factor, at least in blade coating systems with an applicator roll.

The deformation of the blade during bent blade coating was modeled by Saita and Scriven (*4*). They calculated the deformation of the blade in conjunction with the lubrication flow. An important aspect of the results is that there is a limit to the coat weight range a bent blade can produce. If the loadings increase beyond this limit, the blade deforms to such a point that the geometry starts to change and the coat weight increases instead of decreasing. The analysis explains both experiments and normal operation with the bent blade coater.

Pranckh and Scriven (1990) presented a finite element analysis of the blade coating operation with an applicator roll system (*5*). The full two-dimensional flow field was calculated with free surfaces of the coating being free both upstream and downstream of the blade. The blade deflection was calculated in conjunction with the coating flow. The compression of the paper web was included as a simple spring model, since the substrate deforms locally under local stresses. This model may be good for materials of low Poisson ratio, but it should fail to describe materials such as rubber. The rubber cover is often fifty times thicker than the paper, so any deformation of the fiber web is likely to be small compared to the deformation of the rubber cover.

Chen and Scriven described the penetration of fluid into a compressible porous web during blade coating (*6*). The fluid flow was described by the lubrication theory. The roll coating operation was solved in full, and the blade coating was assumed to use a pressure pulse (*5*). The penetration and compression of air were taken into account as well as the compression of the web, and a local spring model was used to contend with compression.

The influence of a shear-thinning rheology on the fluid flow was reported by Isaksson and Rigdahl

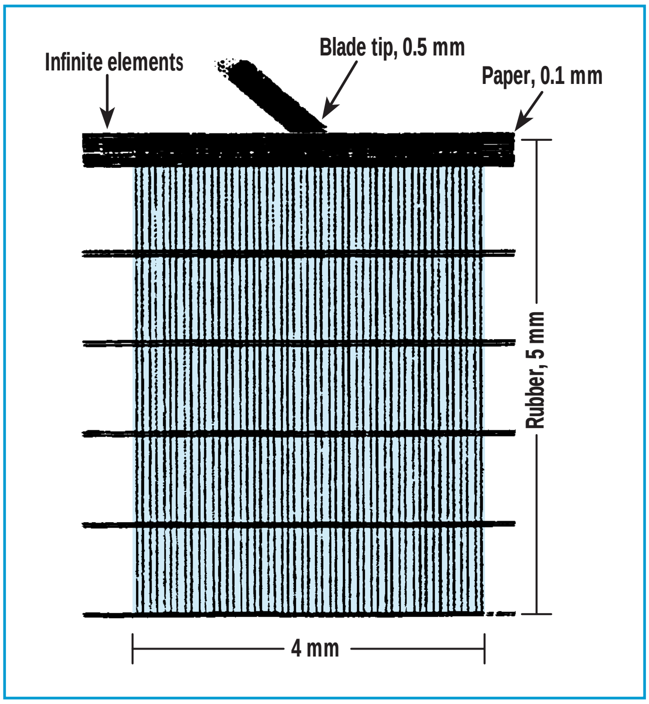

1. Solid mechanics domain and finite element mesh. The top layer is composed of elements with paper properties. The bottom layer is composed of elements with rubber properties.

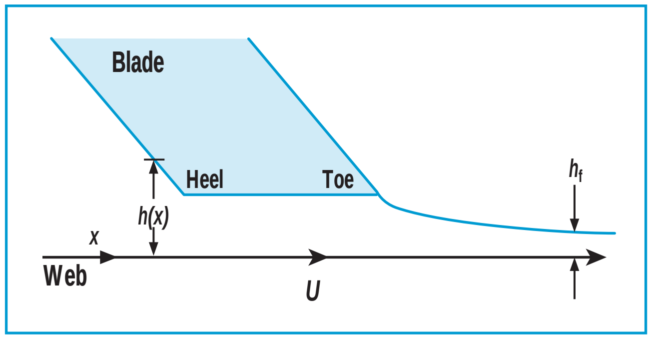

2. Geometry of the fluid flow field. The calculation domain starts 0.5 mm upstream from the blade heel. The distance from the heel to the toe here is held at 0.5 mm.

(*7*). In particular, they analyzed the influence of the rheological properties of the coating fluid on the pressure distribution under the blade. The effect of substrate compression was reported, but the compression geometry and the amount of compression were estimated and were not a result of a calculation. However, the researchers showed that the compression of the substrate has a significant effect on the pressure distribution under the blade.

The hardness of the backing roll has been demonstrated by Ortman and Donigian to influence the uniformity of the coat weight (*8*). This finding indicates that the backing roll does deform during blade coating. In addition, the influence of the paper deformation is minimal compared to the compression of the backing roll in terms of determining the coat weight distribution.

Eklund and Kahila (*2*), Triantafillopoulos and Altug (*9*), Guler and Bousfield (*10*), Isaksson *et al.* (*11*), and others report experimental results of blade coating operations. Often the forces of lubrication flow are estimated based on an assumed geometry. However, these forces can change drastically for small changes in the geometry; in fact, a shift of one degree in the blade angle can cause a doubling of the forces on the blade (*10*). The substrate compression will cause fine features of the geometry to change. This compression must be understood before a good comparison can be made between experimental results and theory. Furthermore, the substrate deformation under the blade also holds implications for the quality of the coated product. Engström and Morin noted that a more pronounced compression of the paper surface can produce a coating layer of a more uniform thickness (*12*).

MODEL DEVELOPMENT

Solid mechanics

The deformation of the paper web and the underlying rubber cover are calculated with a program, ABAQUS, which is based on the finite element analysis. The paper and rubber are assumed to be linear elastic isotropic materials. For example, the strain in the x direction, ε_x, is related to the stress components σ_x, σ_y, and σ_z by the relationship (*13*):

$$\varepsilon_x = \frac{1}{E}\left[\sigma_x - \nu\left(\sigma_y + \sigma_z\right)\right] \qquad (1)$$

where E is the elastic modulus and ν is the Poisson ratio.

Equation 1 and a similar equation for the y direction are solved simultaneously with the stress balances and the compatibility equations. The boundary conditions are described below. The assumptions are that the strain occurs in a plane and that deformation is not dependent on time.

In the calculations, the rubber is assumed to have a thickness of 5 mm, a Young's modulus of 5 MPa, and a Poisson ratio of 0.45. Paper is assumed to have a thickness of 0.1 mm, a Young's modulus of 250 MPa, and a Poisson ratio of 0.05. These values are chosen based on published data. For the solid mechanics, the domain length in the machine direction is 4 mm; this length gives room in front of and behind the blade. The elements in the paper plane are spaced every 20.0 µm in the machine direction. The blade heel is at the center of the domain.

In the calculations, the substrate experiences the pressure pulse from the flow field. The pressure profile is imposed as a stress boundary condition to the top elements in the domain. **Figure 1** illustrates the finite element mesh used to calculate the deformation of the substrate.

In the independent spring model of substrate deformation, the displacement of the web is assumed to

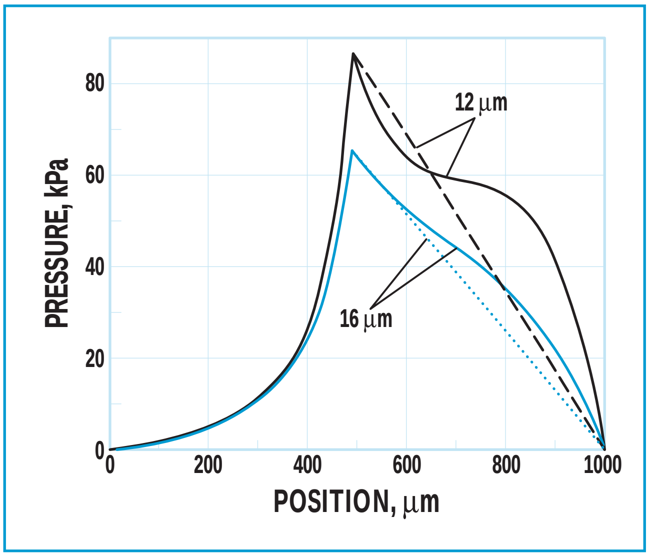

3. Pressure profiles under the blade for 15 m/s and 50 mPa·s fluid for two coating thicknesses of 12 and 16 µm.

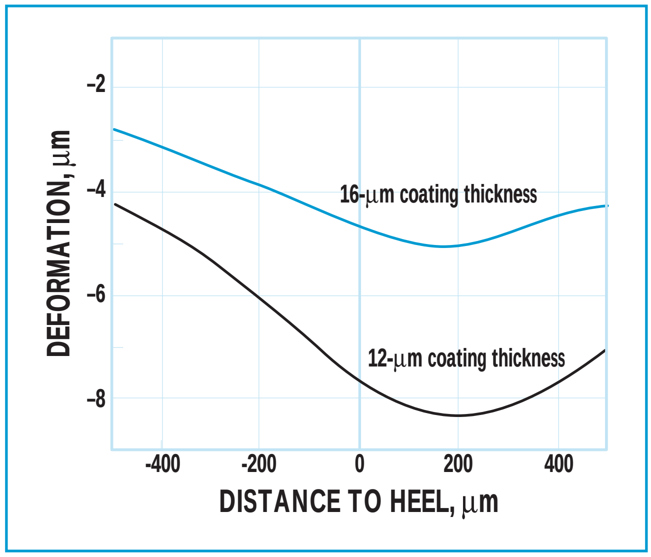

4. Deformation of the substrate for coating thicknesses of 12 and 16 µm, from the finite element calculation.

be proportional to the local stress field. Because the normal stresses (pressure) are larger than the tangential stresses in this case, we assume that the local displacement is proportional to pressure:

$$|z - z_0| = kP \qquad (2)$$

where z is the vertical position of the web surface, z_0 is the undeformed position of the web, k is a spring constant, and P is the local pressure.

This approach is similar to the technique others have used for forward roll coating with deformable rolls (*14*). More complicated models have recently been reported for forward roll coating by Carvalho and Scriven (*15*).

One key assumption made in making the calculations by both the spring model and the finite element model is that the applied stresses are in equilibrium with the deformation. In reality, however, the deformation may lag behind the applied stress. Measuring the dynamic response of the paper–rubber system is possible, and this complication could be added in future analyses of this problem. However, in the results presented here, we have assumed that the deformation is static.

Fluid dynamics

The fluid dynamics are solved using a lubrication analysis. The pressure profile is found by the equation:

$$\frac{\partial P}{\partial x} = -\frac{12 \mu U \left(h_f - \frac{h(x)}{2} \right)}{h(x)^3} \qquad (3)$$

where P is the pressure, x is the position coordinate, µ is the viscosity, U is the web velocity, h_f is the final film thickness, and $h(x)$ is the distance between the web surface and the blade surface. In this description of the flow field, we have assumed that there are no inertial forces, that the fluid is Newtonian, and that there is no porosity of the web.

Equation 2 is integrated numerically, given a shape factor $h(x)$, to obtain the pressure distribution. The pressure boundary conditions are the atmospheric pressures at the inlet position (0.5 mm upstream of the heel) and at the outlet position (the toe). The pressure distribution is integrated to obtain the blade force.

Figure 2 shows the geometry of the fluid flow and the coordinate system. The top surface of the web is the lower boundary of the figure. The web moves with velocity U, and it deforms downward. When the web deforms, the shape function $h(x)$ is modified.

If stagnation pressure is included as an inlet pressure condition, the lubrication analysis is adequate in describing the pressure distribution, compared to a full two-dimensional analysis for roll applicator systems (*16*). Guler and Bousfield demonstrated that the lubrication analysis without the stagnation pressure is accurate for pond systems, and the solutions compare well with the full two-dimensional analysis (*10*). No stagnation pressure is imposed in the calculations presented here.

Though the influences of operational parameters are explored for many different values, typical parameters are a web speed of 15 m/s, a viscosity of 50 mPa·s, and a coating thickness of 12 µm. The blade was always at a 45° inlet angle, and it ran parallel to the undeformed web, as illustrated in Fig. 2. The upstream distance from the inlet to the heel and from the heel to the toe are both 0.5 mm. The blade position had to be adjusted relative to the undeformed substrate to obtain certain coat weights.

In the finite element model, the pressure pulse, $P(x)$, from the lubrication analysis acts as a boundary condition for the top surface of the paper web; in the spring model, it determines the spring deformation.

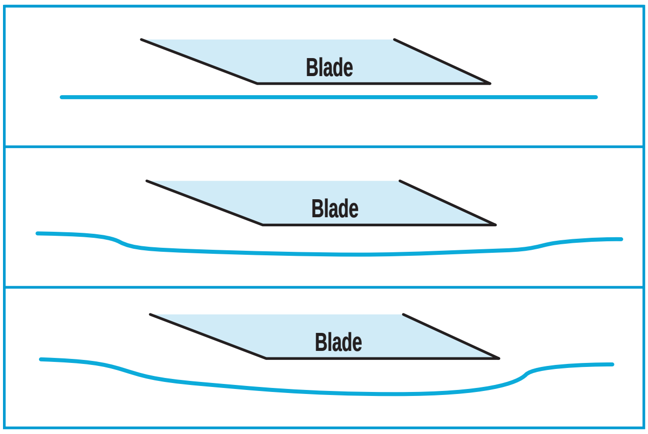

5. Increased deformation of the web and rubber roll.

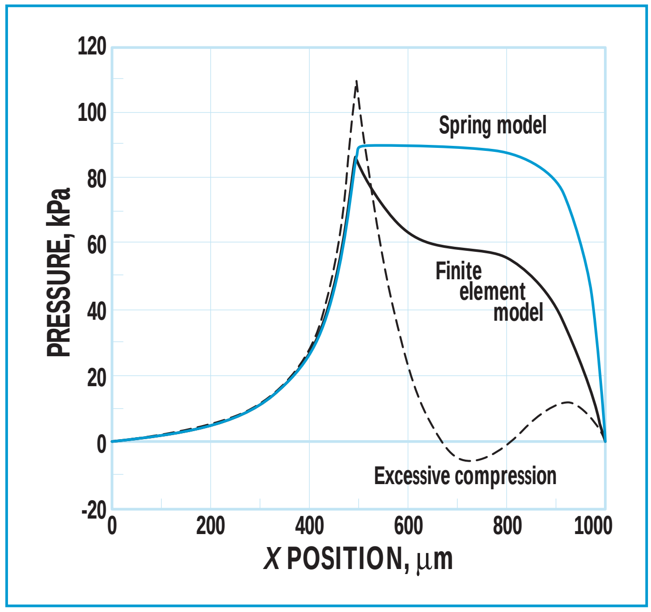

6. Comparison of the spring model and the finite element model for substrate compression for a 12-µm coating thickness with a velocity of 15 m/s and a viscosity of 50 mPa·s.

The pressure boundary condition determines the amount of deformation. The deformation of the substrate determines the geometry for the lubrication analysis through the shape function *h*(*x*). Solutions are obtained with a "Picard"-type iteration between the two calculations until there is less than a 4% change in values. The spring model of deformation works in the same manner except that the deformation at each location is a simple relationship, which is given in Eq. 2.

The results from the calculation are the pressure or stress distribution in both the liquid and the solid, the amount of substrate deformation, and the coat weight. The blade position, relative to the undeformed web, is adjusted vertically to obtain a specified coat weight.

RESULTS

Figure 3 shows the calculated pressure pulses required to obtain coating thicknesses of 16 µm and 12 µm for both an undeformed web (broken lines) and a deformed web (solid lines). We calculated the deformation using the finite element model.

KEYWORDS
Blade coating, deformation, finite element analysis, fluid dynamics, fluid flow, fluid mechanics, paper webs, pressure, rubber rolls.

When the substrate does not deform, the pressure decreases linearly between the heel and the toe of the blade, as others have reported (*5*). However, when the substrate is allowed to deform, the pressure pulse develops a shoulder near the toe of the blade. This shoulder arises because the nip converges near the toe as the paper and rubber roll exit from under the blade. This development is more pronounced for lighter coat weights, where this shoulder develops into a second pressure pulse. **Figure 4** contains the deformation information for the two coat weights calculated by the finite element method.

An interesting result is obtained when the blade forces are compared for the deformed and undeformed pressure profiles. The force on the blade increases as the substrate is allowed to deform. This force increases from 29.8 to 34.5 N/m for the 12-µm coating thickness when deformation is included in the calculation. The force increases from 23.4 to 24.1 N/m for the 16-µm coating thickness as the substrate is allowed to deform. These results are in keeping with other results in the pertinent literature, such as the results for roll coating with deformable rolls reported by Carvalho and Scriven (*17*). The general result is that a substrate of softer rubber will increase the force on the blade needed to obtain the same target coat weight.

Figure 5 illustrates the situation as the web and roll cover deform. A converging channel will build up pressure, while a diverging channel will cause pressure to decrease. The top figure shows the undeformed case. The converging channel causes pressure to increase to the heel of the blade, but the pressure decreases linearly in the parallel channel.

The middle drawing represents the start of a pressure shoulder near the toe as the deformation increases. This shoulder in the pressure profile forms near the toe because there is a converging region just in front of the toe of the blade. In this region, the substrate and the toe tend to converge.

The bottom configuration shows a diverging region after the heel of the blade. This deformation leads to a decrease in pressure and a limit to stable solutions.

Figure 6 illustrates the pressure profile obtained when the deformation increases further, as in the bottom of Fig. 5. The shoulder in the pressure pulse develops into a second pressure peak. This development is caused by the following situation.

As the pressure increases near the toe, the deformation increases near the toe. The increased deformation in this region leads to a diverging region after the heel. Because the clearance is close between the web and the blade, the lubrication forces cause the pressure to decrease in a short distance right after the heel of the blade. This decrease can lead to a subambient pressure. Because the normal force on the blade is equal to the integration of the pressure pulse, the force on the blade decreases. This decrease in force on the blade results in less deformation of the roll.

For this situation, no steady solution is possible as far as we can tell. There are conflicting demands on the fluid mechanics and the solid mechanics. The increased deformation generates a diverging region after the heel of the blade, which leads to a negative pressure pulse, lower forces, and less deformation. An unsteady situation must arise when these process conditions are met.

On an industrial scale, the conditions for this unsteady situation are different than in our calculations. Because of the porous nature of the paper web, air can be trapped or transported in the web. This air may act to soften the pressure pulse. In addition, the time-dependent deformation and the water-induced softening of the web will affect the deformation in a somewhat different way than we assumed for our calculations. However, this situation could arise in the mill for higher speeds or blade loadings. The lubrication equations can be modified to account for the porous nature of the web (*6, 16*).

Figure 6 compares the pressure distributions required to obtain a 12-μm coating thickness as calculated by using either the finite element model or the spring model. Also shown is the pressure distribution that corresponds to an excessive compression, as calculated with the finite element model.

One point should be made: a simple spring model of the deformation is not adequate for larger deformations because of the rubber's high Poisson ratio and the planar propagation of stresses. In the spring model, the substrate deforms locally to adjust to the local pressure, while the finite element model gives a smooth deformation that is proportional to the total force of the blade.

Neither the second peak nor the shoulder in the pressure profile near the toe is obtained with the spring model. The reason is that the solid can deform locally to accommodate the pressure, which creates a situation where a single pressure plateau extends under the blade channel. The feature at the heel of the blade in the pressure profile for the spring model demonstrates the physically unrealistic results from this model. However, the spring model is useful for giving a first impression of the physics.

The spring model also has limits as to the amount of deformation that can be modeled with it. As the deformation increases with the spring model, the pressure pulse becomes constant under the blade tip, as in Fig. 6. The channel deforms uniformly in this region. However, the pressure boundary condition needs to be met at the toe, and the pressure and deformation must be zero at this point. As the deformation increases, conflicting demands are placed on the spring system and the fluid dynamics in this region. Solutions cannot be found for parameters that lead to large deformations.

When an excessive compression occurs, a critical operating condition is approached. The parameters that determine this operational limit are the web velocity, the coating viscosity, the final fluid film thickness, and the elastic modulus of the rubber. These parameters can be put together into a single dimensionless group, an elasticity number N (*15*):

$$N = \frac{\mu U}{h_f E} > 0.015 \qquad (4)$$

The value of 0.015 is a result of three critical conditions that we found for two different viscosities and speeds. This relationship combines the influences of the various parameters into a single expression.

This equation explains that more compression will occur as the viscosity or web velocity is increased or as the coat weight or the rubber hardness is decreased. If the combination of these parameters exceeds 0.015, then an excessive compression occurs, and steady solutions to the set of equations do not seem to be possible.

This condition is valid only for the inlet geometry defined here and a blade running parallel to the web. Again, the industrial situation will be different because of the porous web and the viscoelastic behavior of the substrate. However, a similar combination of parameters could probably be used to characterize the industrial limits.

CONCLUSIONS

The calculation of the substrate compression and the pressure distribution under the blade reveals a complex behavior during blade coating. Small deformations cause the pressure pulse to broaden and form a shoulder near the toe of the blade. This result produces a larger blade loading needed to obtain the same coat weight as that obtained in the undeformed case.

As deformation increases, a double pressure pulse begins to form, one pulse at the heel of the blade and one at the toe. Increased deformation leads to a case where no steady solution is possible, because conflicting demands are placed on the solid and fluid mechanics. These process conditions may explain some coat weight limits of blade coaters. The spring model of substrate deformation is found inadequate in describing deformations over 5 μm because of the importance of the fine features of the geometry in this flow situation.TJ

Bousfield is a professor in the Paper Surface Science Program, Dept. of Chem. Eng., University of Maine, Orono, ME 04469. Rigdahl is a professor, and Wikström is a project area manager at the Swedish Pulp and Paper Research Institute, STFI Box 5604, S-114 86 Stockholm, Sweden.

This work was supported by the industrial sponsors of the University of Maine Paper Surface Science Program and by the sponsors of STFI.

Received for review Feb. 5, 1997.
Accepted Oct. 27, 1997.

Presented at the TAPPI 1997 Coating Conference.

LITERATURE CITED

1. Turai, L. L., *Tappi* 54(8): 1315(1971).
2. Eklund, D. and Kahila, S. J., *Wochbl. Papierfabr.* 106: 661(1978).
3. Kuzmak, J. M., *Tappi J.* 69(2): 72(1986).
4. Saita, F.A. and Scriven, L. E., *1985 Coating Conference Proceedings*, TAPPI PRESS, Atlanta, p. 13.
5. Pranckh, F. R. and Scriven, L. E., *Tappi J.* 73(1): 163(1990).
6. Chen, K. S. A. and Scriven, L. E., *Tappi J.* 73(1): 151(1990).
7. Isaksson, P. and Rigdahl, M., *Rheol. Acta* 33: 454(1994).
8. Ortman, B. J. and Donigian, D. W., *1992 Coating Conference Proceedings*, TAPPI PRESS, Atlanta, p. 217.
9. Triantafillopoulos, N. G. and Altug, N., *1994 Coating Conference Proceedings*, TAPPI PRESS, Atlanta, p. 77.
10. Guler, E. and Bousfield, D. W., *1995 Coating Conference Proceedings*, TAPPI PRESS, Atlanta, p. 53.
11. Isaksson P., Engström, G., and Rigdahl, M., *Nordic Pulp Paper Res. J.* 3: 150(1994).
12. Engström, G. and Morin, V., *1995 Coating Fundamentals Symposium*, TAPPI PRESS, Atlanta, p. 41.
13. Timoshenko, S., *Theory of Elasticity*, McGraw-Hill, New York, 1934.
14. Coyle, D. J. *Chem. Eng. Sci.* 43: 2673(1988).
15. Carvalho, M. S. and Scriven, L. E., *1994 International Printing and Graphic Arts Conference Proceedings*, TAPPI PRESS, Atlanta, p. 259.
16. Bousfield, D. W., *Tappi J.* 77(7): 161(1994).
17. Carvalho, M. S. and Scriven, L. E., *Tappi J.* 77(5): 201(1994).